Polymer 54 (2013) 2706–2716

Contents lists available at SciVerse ScienceDirect

Polymer

journal homepage: www.elsevier.com/locate/polymer

Microstructure characterization through mechanical, electrokinetic and spectroscopic methods of polyampholyte gelatin hydrogels crosslinked with poly(vinyl alcohol)

Andrea Porcaro, Mariel L. Ottone, Julio A. Deiber*

Instituto de Desarrollo Tecnológico para la Industria Química (INTEC), Universidad Nacional del Litoral (UNL), Consejo Nacional de Investigaciones Científicas y Técnicas (CONICET), Güemes 3450, 3000 Santa Fe, Argentina

ARTICLE INFO

Article history:
Received 14 December 2012
Received in revised form
13 March 2013
Accepted 22 March 2013
Available online 2 April 2013

Keywords:
Gelatin-poly(vinyl alcohol) hydrogel characterization
Hydrogel mechanical properties
Hydrogel electrokinetic properties

ABSTRACT

The microstructure of polyampholyte gelatin hydrogels crosslinked covalently with fully hydrolyzed poly(vinyl alcohol) is characterized. The experimental methodology involves simple mechanical extension, spectroscopic and thermal methods (FTIR, XRD, DSC, TGA) and equilibrium swelling test to quantify relevant microstructural parameters and electrokinetic properties of this polyampholyte-polypeptide hydrogel, for a well defined range of crosslinker to gelatin mass ratios. These polyampholyte crosslinked matrices having different positive effective electrical charge are studied within an experimental and theoretical framework of their elastic and swelling properties. Estimations of average mesh size and toughness of the swollen hydrogels are provided. The feasibility of polyion complexation between positive crosslinked gelatin chains and negative bioactive macromolecules to be delivered through hydrogel biodegradation is analyzed. Several additional hydrogel properties are estimated like shear modulus, average molecular mass of network strands, swelling ratio, Flory–Huggins interaction parameter, hydrogel electrostatic zeta-potential and average effective charge number per chain before and after the crosslinking process to quantify gelatin chain cationization.

1. Introduction

Different types of water soluble gelatins are obtained through acid and alkaline hydrolysis processes by denaturing the structures of native collagens. Consequently, via the triple helix tropocollagen degradation, polydisperse gelatin chains are obtained [1–3]. Gelatins are well known for their non-toxic, non-irritant and biocompatible properties, and they are widely utilized in food, biomedical, biotechnological and pharmaceutical industries [2].

At present quantitative procedures to characterize electrically charged matrices of crosslinked gelatin chains through mechanical and physicochemical techniques are required [4]. These hydrogels are used in the controlled release of polyampholyte-polypeptide bioactive chains which are previously loaded in the electrically charged matrix through polyion complexation [5–12] and then released mainly via enzymatic degradation *in vivo* at the desired site [13,14]. This mechanism indicates that either positive or negative charged gelatins interact ionically with opposite charged drugs to form polyion complexes.

There are several studies indicating the relevant functions of gelatin hydrogels in many applications. One case is for instance the sustained release of growth factor exerting effective biological functions like the induction of neovascularization and regeneration of bond cartilage and nerves [15–20]. Also for controlled release purposes, gelatin hydrogels have been applied clinically in gene therapy to treat cancer and congenital immunological diseases. The achievement of the *in vivo* controlled release of a plasmid DNA from a biodegradable gelatin hydrogel enhanced significantly the expression of this macromolecule around the implanted site [21,22].

This work considers specifically the characterization of block matrix gelatin hydrogels (implant matrices) where the quantification of matrix cationization for drug polyion complexation is important. In general, the performance of gelatin hydrogels for controlled drug release depends mainly on [7] (i) the degree of the chemical crosslinking of either basic or acidic gelatin, (ii) the matrix electrical state relating to positive or negative effective electrical charges of chains before and after the crosslinking process, and (iii) the rate of matrix enzymatic biodegradation and hydrolysis *in vitro* and *in vivo* releasing polyampholytic drugs. Here we are concerned

* Corresponding author. Tel.: +54 0342 4559175/77; fax: +54 0342 4550944.
E-mail address: treoflu@santafe-conicet.gov.ar (J.A. Deiber).

0032-3861/$ – see front matter © 2013 Elsevier Ltd. All rights reserved.
http://dx.doi.org/10.1016/j.polymer.2013.03.045

with (i) and (ii). In relation to point (iii), the preservation of biological activity of proteins released from gelatin hydrogels has been analyzed in Refs. [7,8] and citations therein. In this framework, one observes that gelatins in aqueous solution may be covalently crosslinked by different small bifunctional molecules or polyfunctional macromolecules [23–29] which bind either amino or carboxylic groups of amino acid residues of polypeptide chains, generating crosslinks like −N═CH− and −COOC−. At present it is clear that gelatin hydrogels have the advantages of presenting biocompatibility and biodegradability with an innocuous nature response in biological applications and pharmacological formulations [7,12,15]. Nevertheless, concerns are mainly in relation to the citotoxicity produced by the type of crosslinker used that could remains in the matrix. For instance free glutaraldehyde (GTA) used as crosslinker has a certain degree of cytotoxicity and hence successive washes of the hydrogel formed are necessary. Other alternative is to use poly(vinyl alcohol) (PVA) as crosslinker, which is also a water soluble, non-toxic, synthetic polymer. This strategy is substantially different from that using PVA as the basic macromolecule to obtain electrically neutral hydrogel matrices (see Refs. [30–35] and citations therein). In fact, within this challenging framework, the present work proposes the mechanical and electrokinetic characterization of gelatin hydrogels crosslinked with polyfunctional PVA. Therefore, the range of PVA concentrations is chosen to fulfill the role of crosslinker only, and also with the purpose of keeping the expected characteristic and functionality of the polyampholytic-polypeptide gelatin chains in a polyion complexation process as indicated above.

This work is organized as follows. In Section 2, the characteristics of the pig-skin-gelatin (PSG) and PVA polymers used are evaluated and analyzed. They are required as input data in the theoretical framework developed in the following sections. Then experimental methods are briefly presented. A mechanical test involving stress response in simple extension and swelling quantifications follow details described in Ref. [4]. In addition, hydrogel experimental studies are carried out through FTIR, XRD, DSC and TGA. In Section 3.1 theoretical analyses concerning experimental results of the mechanical test are presented, based mainly on hyperelastic stress constitutive models associated with typical elastic energy functions [36,37]. Further useful considerations of the shear modulus in relation to microstructural parameters are provided. In Section 3.2 the swelling theory of PSG−PVA crosslinked charged matrices is considered. Section 4 analyzes and discusses experimental results and numerical evaluations. Finally main conclusions establishing the relevance of some characteristic parameters obtained for crosslinked PSG−PVA hydrogels are provided like, matrix shear modulus G, average molecular mass M_c of network strands, average matrix mesh size ξ, swelling ratio Q_e, average polypeptide−aqueous solvent Flory−Huggins interaction parameter χ, hydrogel electrostatic zeta-potential ζ and average effective charge numbers per chain before Z and after Z_p the crosslinking process, respectively. Concerning hydrogel effective charges, significant differences between polyampholyte and polyelectrolyte chains forming hydrogels exist, mainly in relation to their possible conformations and electrokinetic properties in the crosslinked network. In these regards polyampholyte hydrogels were less studied (see Ref. [4] and citations therein).

2. Materials and methods

2.1. Basic properties and description of PSG

A PSG sample purchased from Sigma Chemical Company was used (average molecular mass $M_{PSG} \approx 80$ kDa, bloom value 300 g, isoelectric point pI ≈ 8 and density $\rho_{PSG} = 1.369$ g/cm^3). Since the PSG chain properties depend on the fabrication chemical process, approximate values Z per average chain as a function of pH are required in order to estimate the hydrolysis suffered by the amino acid sequence (AAS) of the native tropocollagen units, which must be compatible with the pI value. Here the calculation of pI is carried out by following the procedure reported in Ref. [4]. It was thus found that this PSG sample has a degree of conversion around 43.42%, which is a typical value for pI ≈ 8 (see Supplementary data). Therefore the average effective charge of gelatin chains is $Z \approx 0.656$ (small effects associated with the "charge regulation phenomenon" [4] are neglected in Table S1). Based on results reported in Table S1, the average molecular mass of amino acid residues composing the PSG sample is $M^m_{PSG} \approx 91.01$ Da. Therefore, the total number of amino acid residues is $N \approx 879$, and the number of −COOH groups of Asp and Glu amino acid residues estimated in the average PSG chain is $X \approx 71.7$. These groups are available to crosslink −OH of PVA chains.

2.2. Basic properties and description of PVA

A PVA sample fully hydrolyzed was purchased from Sigma Chemical Company having an average molecular mass $M_{PVA} \approx 85$ kDa. This semi-crystalline polymer was used as the crosslinking agent of PSG chains. The PVA is a synthetic macromolecule having a zig-zag planar structure, in which each monomer with molecular mass $M^m_{PVA} \approx 44$ Da has a hydroxyl residual group [32,33,35,38]. This polymer is soluble in water. Also $\rho^a_{PVA} \approx 1.269$ g/cm^3 is the amorphous phase density while $\rho^c_{PVA} \approx 1.345$ g/cm^3 is the crystalline phase density.

2.3. Stoichiometry of the esterification chemical reaction

The basic structure of the PSG−PVA hydrogel is generated through an esterification chemical reaction where hydroxyl groups of PVA react in the presence of a strong acid with carboxyl groups of Asp or Glu amino acid residues of PSG [27]. In this regard, the preparation of the PSG−PVA hydrogel is quite different from that used to obtain classical gelatin-GTA hydrogels [39]. To visualize this aspect, the comparison of Fig. 1 here and Fig. 1 in Ref. [4] is relevant. In fact, the

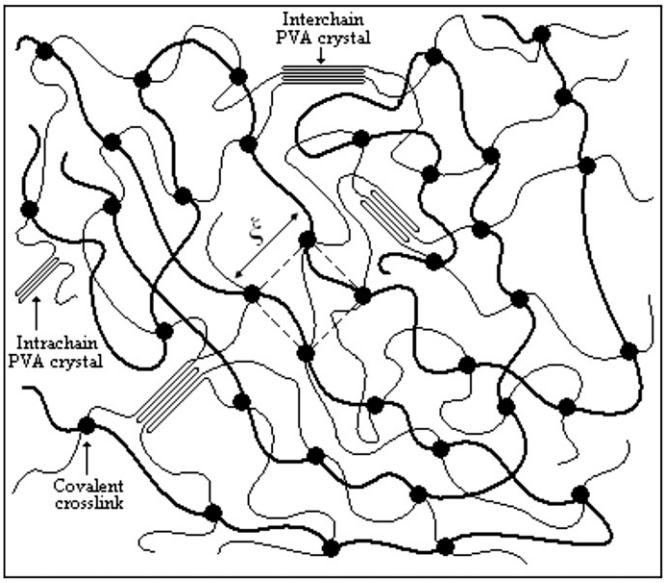

Fig. 1. Scheme illustrating a gelatin hydrogel crosslinked with poly(vinyl alcohol). Thin (−) and thick (−) lines refer to PVA and PSG chains, respectively. Dashed lines delimit an idealized region of the network scaled through the average mesh size.

esterification reaction to form PSG–PVA hydrogels is carried out in a strongly stirring batch at 70 °C. Physical bond formation in the final matrix due to partial reversion of tropocollagenic triple helix is neglected as explained and validated in Section 4.1.

Since crystallites are formed with PVA in the film casting process (Section 2.4), this discrete phase must be accounted as part of the polymeric matrix in the hydrogel characterization process (Fig. 1). Also from the extensional test and the rubber elasticity theory [4] the minimum number of covalent sites X_C between PSG and PVA chains may be estimated as follows,

$$X_C = \left(\frac{M}{M_c} - 1\right) \tag{1}$$

In Eq. (1), the terminal –COOH groups in the PSG chain are taken as elastically non-effective crosslinks, yielding end defects in the network. Here $M = x_{PVA}M_{PVA} + x_{PSG}M_{PSG}$ is the average number molecular mass of chains in the hydrogel, where x_{PVA} and x_{PSG} are the PVA and PSG molar fractions, respectively. Consequently, parameter X_C allows one the evaluation of the maximum average number X_E of –COOH sites per gelatin chain remaining without forming a covalent crosslink. Thus the minimum effective electrical charge of the gelatin chain after the crosslinking process is $Z_p = Z + X_C$. On the other hand, FTIR is used as described below for the actual determination of X_C, X_E and Z_p. It is clear that quantities like N, X, X_C and X_E are integer values although calculations must be carried out considering them as real numbers (see discussion in Ref. [4]).

2.4. Hydrogel preparation

All the PSG–PVA hydrogels were prepared through the following protocol [27]. An aqueous solution of PVA was obtained by dissolving the suitable mass m_{PVA} of PVA in distilled water at 90 °C. Then a weighed mass m_{PSG} of gelatin required to obtain a specific formulation was dissolved in the PVA solution at 70 °C to yield 100 ml of total solution. Finally, 0.05 ml of concentrated hydrochloric acid (HCl 35%) was added, and the resulting dispersion was strongly stirred at 70 °C for half-hour to carry out the esterification reaction. The rather viscous dispersion obtained was used to produce a thin hydrogel through the conventional casting procedure at room temperature. After 30 min the resulting film was washed thoroughly with distilled water to remove the remaining HCl. At this stage, the swelling ratio $Q_o = V_o/V_p$ was determined for each PSG–PVA hydrogel formulation by following the procedure in Section 2.5 below. Here, V_o is the volume of the relaxed hydrogel after covalent bonds are formed, and V_p is the volume of the dry sample [4,40] (Section 2.5). All samples washed at room temperature are then dried at 8 °C for around 7 days before they are used in swelling and mechanical tests.

Since one of the purposes of this work is to evaluate the performance of the PVA as a polyfunctional crosslinker of the PSG biopolymer, three hydrogel sets were formulated. In Set I the ratio $r = m_{PVA}/m_{PSG}$ was kept constant at $r = 1$. In Set II this ratio was $r = 4$. In Set III the PSG concentration was fixed at 5% w/w while the PVA concentration was varied from 10 to 17.5% w/w. The hydrogels studied were coded H-1 to H-11 as indicated in Table 1. Further, since masses m_{PVA} and m_{PSG} are in a solution batch of 100 ml, r also defines the ratio of PVA to PSG concentrations in g/100 ml throughout this work.

2.5. Swelling tests

For swelling tests, dry hydrogel strips were immersed in physiological solutions (pH 7 and ionic strength I = 150 mM) until the equilibrium between the swollen film and solution was achieved at around 72 h. This condition corresponded to a time independent swelling ratio $Q_e = V_g/V_p$ as a function of immersion time. Here V_g is the volume of the swollen sample once the equilibrium is achieved. For this purpose the amount of absorbed water in the hydrogel was determined by the difference between wet W_w and dry W_d strip weights [4,39]. An Ohaus analytical balance, Adventurer TM model, with a readability and repeatability of 0.1 mg was used. The value of the crosslinked heteropolymer matrix density required was estimated through the following expression,

$$\rho_p = \rho_{PSG}\phi_{PSG} + \rho^a_{PVA}\phi^a_{PVA} + \rho^c_{PVA}\phi^c_{PVA} \tag{2}$$

where $\phi_{PSG} = 1/\{1 + r\rho_{PSG}(f_a/\rho^a_{PVA} + f_c/\rho^c_{PVA})\}$, $\phi^a_{PVA} = (f_a r)/\{\rho^a_{PVA}/\rho_{PSG} + r(f_a + f_c\rho^a_{PVA}/\rho^c_{PVA})\}$ and $\phi^c_{PVA} = (f_c r)/\{\rho^c_{PVA}/\rho_{PSG} + r(f_a\rho^c_{PVA}/\rho^a_{PVA} + f_c)\}$ are the PSG and amorphous and crystalline PVA volume fractions in the dry hydrogel, respectively. Also f_a and f_c are the amorphous and crystalline PVA mass fractions normalized with m_{PVA}. Since the network swelling process does not affect the crystalline parts of PVA chains[41], Eq. (2) permits the calculation of the hydrogel swelling ratio through,

$$Q_e = 1 + (W_w - W_d)\rho_p/(W_d\rho_w) \tag{3}$$

where ρ_w is the density of the physiological solution used in swelling tests. Similar procedures were used to determine Q_o and Q_{aw} (Table 1). Here Q_{aw} is the hydrogel swelling ratio when a water-ethanol solution in the ratio 2:3 with density $\rho_{aw} = 0.873$ g/cm^3 is used to plasticize the hydrogel sample before mechanical tests (Section 2.7). In swelling experiments at least three samples were tested for each type of hydrogel. Measurements are reported in Table 1 by including maximum standard deviations.

2.6. Spectroscopic and thermal tests

Throughout this work reference to mixture samples M-1, M-7 and M-8 (one per hydrogel sets) implies the raw hydrogel formulations H-1, H-7 and H-8 without crosslinks; thus, the catalyst HCl is not added. Pure PVA and PSG, and both hydrogel and mixture samples were studied via Fourier transform infrared (FTIR) (Perkin–Elmer, Spectrum One) and X-ray diffraction (XRD) (Seifert model, JSO Debyeflex-2002) spectroscopic methods with the

Table 1
Experimental crystalline PVA mass fraction f_c in hydrogels and PSG–PVA hydrogel swelling ratios Q_o, Q_{aw} and Q_e for samples H-1 to H-11. f_c values are obtained from XRD diffractograms (see also table footnote). All swelling ratios were repeated three times for each sample giving maximum SD = ±0.3, 0.2 and 0.2 for Q_o, Q_{aw} and Q_e, respectively. Also $r = m_{PVA}/m_{PSG}$, where m_{PSG} and m_{PVA} are the PSG and PVA masses used in 100 ml of solution to produce the crosslinked matrix (Section 2.4).

Hydrogel code	m_{PSG} (g)	m_{PVA} (g)	r	f_c(%)	Q_o	Q_{aw}	Q_e
Set I							
H-1	2.5	2.5	1	27.6[a]	19.8	4.6	12.4
H-2	5	5	1	40.0	10.6	3.7	11.8
H-3	10	10	1	43.6[a]	4.5	2.6	7.3
H-4	12.5	12.5	1	47.3[a]	4.3	2.6	6.1
Set II							
H-5	1.25	5	4	46.9	15.5	2.3	5.1
H-6	2.5	10	4	50.0	7.7	2.1	4.1
H-7	3	12	4	51.8	6.2	2.2	4.0
Set III							
H-8	5	10	2	49.6	6.7	2.5	4.9
H-9	5	12.5	2.5	58.1	6.0	2.4	4.2
H-10	5	15	3	59.6	5.5	2.4	3.9
H-11	5	17.5	3.5	59.9	5.2	2.2	3.8

[a] f_c obtained from DSC tests gives values around 30.1, 43.2 and 52.9% for H-1, H-3 and H-4, respectively (see Section 4.1).

following three purposes: (A) The crystalline mass fraction of pure PVA film is estimated via FTIR through $f_c^o = A(1141)/A(2920)$, where the absorbance of C–O forming hydrogen bonds in the PVA crystals is at 1141 cm^{-1} [32,42] while the associated C–H absorbance (invariant amount of stretching atom pair in the PVA backbone chain) is a neat peak at 2920 cm^{-1} within the range 3000–2850 cm^{-1} as depicted in Fig. 2. The one-to-one ratio of C–H and C–O in the primary configuration of PVA is used. Here a super script (^{o}) stands for pure PVA.

The estimation of crystalline PVA mass fractions in pure, mixture and hydrogel films are obtained via XRD tests. All films are formed through the same process. Thus since the intensity of PVA crystal diffraction $I_c(2\theta)$ at $2\theta \approx 20^\circ$ is a measure of PVA crystallinity [43–46], one obtains $f_c = I_c(20^\circ)/(I_c(20^\circ)+I_a(20^\circ))$, where $I_a(20^\circ)$ is the diffraction intensity of the non-crystalline material [47,48] (see Table S2 and Figure S1 (a) and (b)). We have also calculated f_c through peak areas instead of peak intensities obtaining very close results (see procedures and details in Ref. [48]). (B) The X value is estimated from the FTIR spectrum of pure PSG film through $X/N = A(\nu)/A(3328)$, where the N–H absorbance of amide is at 3328 cm^{-1} (invariant amount of stretching atom pair in the PSG backbone chain) while the absorbance $A(\nu)$ of C=O pertaining to carboxylic acids is at a wave number ν comprised between 1725 and 1700 cm^{-1} (stretching of C=O of amide-I is also in this range at 1650 cm^{-1} [49,50], see Fig. 2). We found that $X \approx 72.5$ at $\nu \approx 1718$ cm^{-1} (Section 4), which is close to the theoretical value estimated from the sum of $n_{Glu} \approx 40.2$ and $n_{Asp} \approx 31.5$ reported in Table S1. (C) The crosslink number X_C values are obtained from FTIR spectra (Fig. 3) through $A^M(1718)/A^H(1718) = X/(X - X_C)$, where $A^H(1718)$ and $A^M(1718)$ are absorbances at 1718 cm^{-1} of hydrogel and its corresponding mixture, respectively, involving C=O stretching of carboxylic groups present in PSG amino acid residues Asp and Glu (see Section 2.1). X_C values obtained from this expression are discussed in Section 4.5.

For crosschecking purposes of XRD tests concerning the existence of PVA crystallites in hydrogels, a Mettler Toledo differential scanning calorimeter (DSC) was used to test three films. Dry hydrogel samples were placed in an hermetically sealed aluminum pan and heated at a rate 5 °C/min, between 35 and 290 °C, in an inert environment (100 ml/min of N_2). The phase transition temperature was estimated from the peak of the temperature profile corresponding to the endothermic heat evolution. Therefore the phase transition enthalpy was calculated as the area under this peak by following the procedure in Refs. [32,33]. Thus the crystalline PVA mass fraction f_c was obtained from a known mass of hydrogel sample (see footnote of Table 1, Figure S2 and Section 4.1). In addition thermogravimetric analyses (TGA) of hydrogels were carried out with a controlled TGA/SDTA 851 instrument, by heating from 30 °C to 320 °C at a heating rate of 5 °C/min under a nitrogen atmosphere with a flow rate of 100 ml/min (see Figure S3 and Section 4.1).

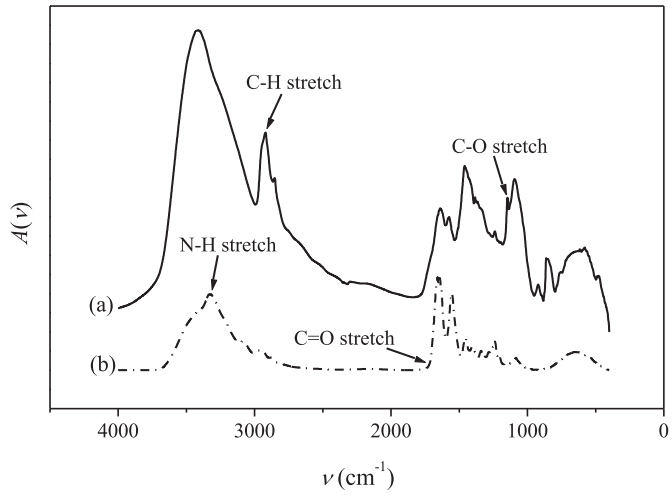

Fig. 2. FTIR spectra of pure PVA (full line) and pure PSG (dash dot line) as a function of wave number ν (cm^{-1}). Arrows indicate the stretching absorbance peaks of atom pairs as follows: (a) C–O forming hydrogen bonds and C–H belonging to –CHOH– along the backbone chain of pure PVA to obtain $f_c^o = A(1141)/A(2920)$, (b) N–H of peptide bonds –CONH– and C=O of carboxylic acids –COOH to obtain $X/N = A(1718)/A(3328)$. Spectrum (a) was normalized according to the peak in the band 3800–3000 cm^{-1} due to free O–H and hydrogen bonded O–H-- stretches. Spectrum (b) was normalized according to the peak in the band 1680–1630 cm^{-1} of amide C=O stretching.

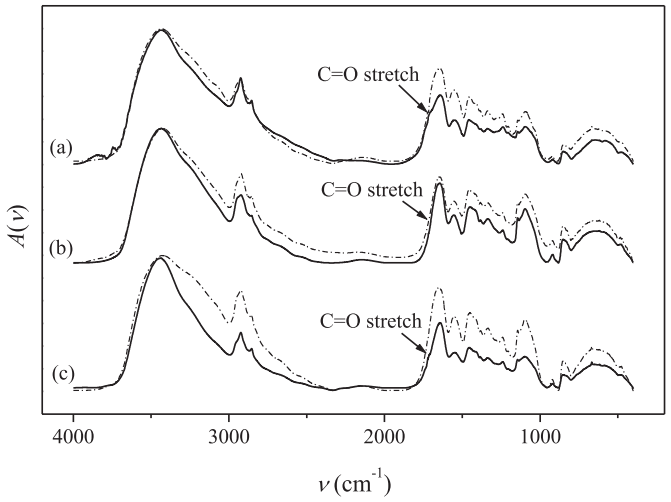

Fig. 3. FTIR spectra of typical hydrogels (full lines) and mixtures (dash dot lines) as follows: (a) H-1 and M-1 with $r = 1$ and $m_{PSG} = 2.5$ g, (b) H-7 and M-7 with $r = 4$ and $m_{PSG} = 3$ g and (c) H-8 and M-8 with $r = 2$ and $m_{PSG} = 5$ g. Arrows indicate the stretching absorbance of carbonyl C=O in carboxyl groups –COOH of Asp and Glu present in hydrogels and mixtures to obtain $X_C = X(1 - A^H(1718)/A^M(1718))$. Spectra were normalized according to the peak in the band 3800–3000 cm^{-1} due to free O–H, hydrogen bonded O–H-- and amide N–H stretches.

2.7. Simple extensional test

Following the procedures in Refs. [4,39] for simple extension tests, hydrogel strips 4 cm long (effective testing length) and 1 cm wide were prepared. Thicknesses were determined with an optical digital caliber (Table 2). Samples were equilibrated in the water–ethanol solution for 72 h to improve their dry deformation by plasticization, and still keeping the appropriate strength for testing. Then by weighing wet and dry strip samples, the swelling ratio $Q_{aw} = V_{aw}/V_p$ was determined, where V_{aw} was the volume of the hydrogel equilibrated with the water–ethanol solution. This ratio is used below to correct the determination of M_c [4]. The plasticized strips were tested in simple extension by using a Shimadzu DSS-10 T-S machine at an axial velocity 5 mm/min. Thus, the axial force as a function of time was recorded and the axial stretch ratio λ was calculated for further analysis. True stress was evaluated by considering the actual cross sectional area of the sample as a function of the axial testing displacement by assuming isochoric deformations. All extensional tests were repeated three times for each sample giving a maximum SD = ± 0.03 MPa.

3. Theoretical considerations

3.1. Stress response of PSG–PVA hydrogels

From the classical rubber elasticity theory (see Refs. [51,52] and citations therein) three basic responses of an elastomeric material under simple extension are usually found, mainly at relatively low

Table 2
Worm-like hyperelastic parameters $G = G_1 + G_2 + G_3$, M_c and β for samples H-1 to H-11 (see Table 1 for hydrogel compositions and Table 3). Also toughness T_H calculated through Eq. (6) and experimental fracture stretch ratio λ_F are provided. Here e_o is the hydrogel thickness and ϕ stands for the PVA crystal volume fraction in the hydrogel plasticized with the water-ethanol solution (Section 2.7). Hydrogel thickness and experimental fracture stretch ratio have an average SD = ±0.006 mm and ±0.19, respectively.

Hydrogel code	e_o (mm)	ϕ	G (MPa)	M_c (Da)	β	T_H (MPa)	λ_F
Set I							
H-1	0.101	0.030	0.038	23,951	0.135[a]	0.065	2.11
H-2	0.231	0.053	0.082	18,215	0.350[a]	0.012	1.31
H-3	0.176	0.083	0.186	12,992	[b]	0.030	1.37
H-4	0.765	0.090	0.156	15,098	[b]	0.030	1.43
Set II							
H-5	0.115	0.162	0.204	10,946	0.038	0.532	2.59
H-6	0.160	0.186	0.780	4662	0.051	2.329	3.59
H-7	0.306	0.188	0.860	4607	0.009	8.040	5.49
Set III							
H-8	0.224	0.127	1.050	3165	0.063	2.197	3.09
H-9	0.301	0.171	1.454	3033	0.018	7.740	5.59
H-10	0.317	0.190	1.480	2877	0.022	7.873	5.24
H-11	0.335	0.201	1.828	2753	0.029	6.679	4.81

[a] BST model also provides a good fitting for H-1 and H-2 with $n = 3.3$ and 4.5, respectively.
[b] Experimental data cover the linear and softening responses only. Eq. (5) reduces to the conventional Mooney model with $G_3 = 0$.

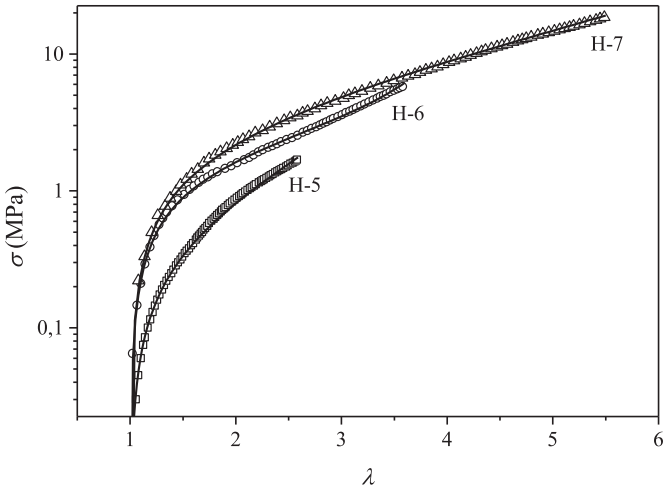

Fig. 4. Normal stress difference σ as a function of stretch ratio λ in simple extension of PSG–PVA hydrogels for $r = m_{PVA}/m_{PSG} = 4$ as follows: H-5 with $m_{PSG} = 1.25$ g (□), H-6 with $m_{PSG} = 2.5$ g (○) and H-7 with $m_{PSG} = 3$ g (Δ). Symbols refer to experimental data obtained from the simple extensional test (Section 2.7). The last experimental point belongs to fracture. Full lines are the best fittings through Eq. (5) for (□), (○) and (Δ). Parameter values for Eq. (5) are reported in Tables 2 and 3. The maximum average fitting error is around 6.7%.

rates of extension. Thus, for low strains the linear elastic response is present, which permits to estimate the shear modulus. This modulus is a function of M_c, and may be also interpreted through different ideal frameworks (see Ref. [52] and citations therein). At intermediate strains a softening response may be observed, which is due to entanglements [52–54]. Finally at relatively high strains, crosslinked chains approach their maximum stretching to get a rather sharp hardening zone before breaking [4]. A sequence of experimental results is depicted in Fig. 4, Figures S4 and S5 concerning the hyperelasticity of PSG–PVA hydrogels in simple extension. These figures indicate that the three zones may be present for this type of hydrogel where a polyfunctional crosslinker is used. The main difference with the elastic response of gelatin-GTA hydrogels [4] is that with a bifunctional crosslinker the softening intermediate zone is not present. Experiments in simple extension indicate that the development of entanglements in PSG–PVA is important as it is validated through the stress difference versus stretch ratio in Fig. 4, Figures S4 and S5. This physical aspect requires a stress constitutive equation different from that used previously in Ref. [4] based on the BST model [36] valid for gelatin-GTA hydrogels.

For PSG–PVA hydrogels, here a "worm-like" hyperelastic model interconnecting the macroscopic stress responses with parameters of the network is used [37]. Therefore for the case of hydrogels exhibiting the three elastic responses described above, we propose the following modified energy function (see also [37]),

$$U = \frac{1}{2}\{G_1(I_1-3)+G_2(I_2-3)+G_3(I_1-3)/[1-\beta(I_1-3)]\} \qquad (4)$$

where, the first and second strain invariants for uniaxial deformation are $I_1 = \lambda^2 + 2/\lambda$ and $I_2 = 2\lambda + 1/\lambda^2$, respectively. In simple extension the normal stress difference $\sigma = \lambda\partial U/\partial\lambda$ is obtained as follows,

$$\sigma = \left(\lambda^2 - 1/\lambda\right)\left\{G_1 + G_2/\lambda + G_3\left[(1-\beta(I_1(\lambda)-3))^{-2}\right]\right\} \qquad (5)$$

In Eq. (5) parameters G_1, G_2 and G_3 are related to the shear modulus G through $G = G_1 + G_2 + G_3$, while $\beta = \langle R_o^2\rangle/{R_{max}}^2$ is the chain elongation ratio for a perfect rubber network [37], where $R_{max} = L_c N_c \cos(w_c/2)$ is the fully extended strand length, and $\langle R_o^2\rangle = L_c^2 C_n N_c$ is the initial relaxed strand length. Here the average Flory characteristic ratio of a strand in this rather complex heterogeneous covalent matrix is estimated from $C_n = \beta N_c \cos^2(w_c/2)$ [37]. Further, the average bond length is $L_c = (x_{PSG}L_{PSG} + x_{PVA}L_{PVA})$ and the average bond number is $N_c = M_c/M_c^m$ where $M_c^m = x_{PSG}M_{PSG}^m + x_{PVA}M_{PVA}^m$ is the monomer average molecular mass associated with M_c. Also L_{PSG} = 3.8 Å and L_{PVA} = 1.54 Å [55] are the characteristic bond lengths of PSG and PVA, respectively. Consequently, we define $w_c = (x_{PSG}w_{PSG} + x_{PVA}w_{PVA})$ as the average angle between two consecutive chain bonds for the planar trans-chain conformation, calculated through the angle $w_{PSG} \approx 74°$ [55] formed by two polypeptide virtual bonds and the angle $w_{PVA} \approx 68°$ for –C–C– bonds in PVA chains. In this framework it is clear that between two consecutive matrix crosslinks, the hydrogels studied here may have either a PVA homopolymer or a PSG heteropolymer strand, generating a substantial complexity to characterize the internal matrix topology. This situation is in part resolved by using appropriate averaged chain properties weighed through number chemical compositions by following consistently hydrogel formulations described in Table 1. From Eq. (5) the hydrogel Hencky toughness T_H in simple extension is readily obtained as follows,

$$T_H = \int_0^{\ln\lambda_F} \sigma d\ln\lambda = U(I_F)$$
$$= \frac{1}{2}\{G_1(I_{1_F}-3)+G_2(I_{2_F}-3)+G_3(I_{1_F}-3)/[1-\beta(I_{1_F}-3)]\} \qquad (6)$$

where the Hencky strain is $\varepsilon_H = \ln\lambda$. Therefore T_H may be evaluated directly from experimental λ_F, once the model parameters in Eq. (5) are available at each hydrogel formulation (lower index F indicates fracture throughout this work).

When the PSG–PVA hydrogels are formulated with relatively low PVA concentration (samples H-1 and H-2 with $r = 1$) the intermediate stress response is not found (see Figure S4, Table 2 and

discussion in Section 4) and the BST model [36] is appropriate for these hydrogels as indicated in Ref. [4]. This model has two parameters only, the constant shear modulus G and the coefficient of strain measure n for isochoric simple extension, and the first normal stress difference is expressed,

$$\sigma = \frac{2G}{n}\left(\lambda^n - \lambda^{-n/2}\right) \tag{7}$$

The BST model yields a Hencky toughness $T_H = 2GI_F/n$ where $I_F = (\lambda_F^n + 2\lambda_F^{-n/2} - 3)/n$ is the first invariant of deformation at fracture [4,36].

In addition G values at each ratio r may be obtained from simple extension tests and correlated with relevant parameters of hydrogel microstructure, like average molecular masses M_c and M, hydrogel density ρ_p and crystal volume fraction ϕ. From the classical rubber elasticity theory [51] one expresses as a first approximation,

$$G = \frac{\rho_p RT}{M_c}\left(1 - \frac{2M_c}{M}\right)\left(\frac{Q_{aw}}{Q_o}\right)^{1/3}\left(1 + 2.5\phi + 14.1\phi^2\right) \tag{8}$$

where R is the gas constant. In Eq. (8) the hydration of the PSG–PVA hydrogel with water–ethanol solution is accounted having as reference the hydration of the relaxed matrix [40]. Also the correction due to terminal chain ends is introduced through the factor $(1 - 2M_c/M)$. The expression $(1 + 2.5\phi + 14.1\phi^2)$ considers the presence of PVA crystallites distributed in the amorphous polymeric matrix assumed as fillers [51] which increases the shear modulus through $\phi = \phi^c_{PVA}/Q_{aw}$. Here ϕ accounts the sample hydration provided by the water-ethanol solution used as plasticizer. The possible crosslinks added by crystallites, which are formed through PVA interchain interactions, are neglected based on the average crystal sizes β_c estimated from Scherrer equation (see discussion in Supplementary data) and XRD experimental results in Table S2. In fact since $\beta_c \approx 40$ Å for H-1 to H-11 samples, the ratio of maximum value of crystal number to crosslink number $rf_cM_{PSG}/(\beta_c^3\rho_c X_c N_A)$ is around 1.7/10 approximately, where N_A is Avogadro constant. This low ratio value justifies neglecting crystallites as crosslinks having rather high size, apart from the fact that PVA chains emerging from crystals have a one-side biased relaxation no contemplated in classical theories. In addition crystals formed by PVA intrachain interactions must be excluded as effective crosslinks. Other hypotheses concerning G in terms of microstructural parameters were discussed in Ref. [4].

By following the experimental procedure, data G, M_c, Q_o, ϕ and Q_{aw} become available. Therefore the number of total elastically effective covalent crosslinks per gelatin chain X_C is obtained through Eq. (1) and the number of effective elastic strands is $(M/M_c)(1 - 2M_c/M)$. Also the hydrogel average mesh size ξ in the swollen state may be estimated, as suggested in the literature [23,56,57]. In this work we use the average mesh size defined in Ref. [4] as follows,

$$\xi \approx 0.704 L_c \left(C_n M_c/M_c^m\right)^{1/2} Q_e^{1/3} \tag{9}$$

where, as a first approximation, a basic ideal strand having M_c/M_c^m peptide bonds is considered.

3.2. Swelling response of PSG–PVA hydrogels

A PSG–PVA crosslinked hydrogel yields a heterochain network that contains positive and negative ionizing groups. This network in contact with a physiological solution (pH 7 and I = 150 mM) reaches a thermodynamic equilibrium after the exchange of free ions and solvent, resulting a swollen polyampholyte network (for a bovine hide gelatin-GTA crosslinked hydrogel see Ref. [4]). The situation involving a swollen polyelectrolyte hydrogel and the surrounding bath was previously described as a Donnan equilibrium where the polymer network acts as its own membrane (see for instance Refs. [51,58–62]) preventing the diffusion of the attached ionizing groups toward the solution bath. In this regard, concerning polyampholyte networks, here we follow Ref. [4] and citations therein. Thus, the study of the thermodynamic equilibrium between hydrogel and physiological solution requires the knowledge of the total free energy change involved in the mixing of the wet formed hydrogel and the formulated solution [4,51,58–62]. This total free energy change is decomposed into (i) the free energy change of the mixing between network and solvent, (ii) the elastic free energy change required to yield the deformed network, and (iii) the mixing free energy change in the network and in the solution bath associated with mobile ions and solvent. Therefore in the present work specific considerations are required: (1) the network swelling process does not affect the PVA crystallites [41]. (2) Since the swelling process of dry hydrogels indicates usually an anisotropic starting matrix, the reference deformation state is taken at the hydrated hydrogel after the crosslinking process and before drying. Thus the change in the network free energy refers to the isotropic hydrogel states with swelling ratios Q_o and Q_e. (3) There are not individual polymer molecules unattached from the network. (4) The lattice theory used in the deduction of entropic free energy considered a uniform cell volume [51], and hence this theoretical hypothesis was also applicable as a first approximation to the particular case of heterochain polymer compound. (5) The affine network model is valid for the change of the network elastic free energy at low λ [4,51,58]. For highly crosslinked hydrogels, non Gaussian effects in chain stretching require an extended version of the basic elasticity theory (see Refs. [62,63] and citations therein). Thus the linear theory applies before the onsets of chain entanglements and/or hardening responses of stress versus stretch ratio, respectively. (6) The swollen hydrogel forms roughly a dilute solution (see also small corrections in Refs. [60,61]). These hypotheses justifies that the total free energy may be expressed as the sum of the basic free energy changes [51]. Therefore, in this framework, one may use approximate expressions of the chemical potentials of mobile ionic species in terms of their concentrations to obtain the condition for solvent equilibrium between swollen hydrogel and solution (see details in Ref. [4]). Thus when the total free energy is minimized, the equilibrium condition involves the balance of osmotic pressures (see also [51] and modifications in Ref. [40]),

$$P_S + P_E + P_I = 0 \tag{10}$$

where,

$$P_E = \frac{RT}{\bar{v}M_c Q_o}\left\{1 - \frac{2M_c}{M}\right\}\left\{\left(\frac{Q_o}{Q_e}\right)^{1/3} - \frac{Q_o}{2Q_e}\right\} \tag{11}$$

is the elastic osmotic pressure,

$$P_S = \frac{RT}{V_1}\left\{\ln\left(1 - \frac{1}{Q_e}\right) + \frac{1}{Q_e} + \frac{\chi}{Q_e^2}\right\} \tag{12}$$

is the entropic osmotic pressure and,

$$P_I = -RT\sum_{i=1}^{N_I} C_i^{\infty}\{\exp(-ez_i\zeta/k_BT) - 1\} \tag{13}$$

is the ionic osmotic pressure. In Eq. (11), Q_e/Q_o is the isotropic stretch ratio of the swollen network referred to the unrelaxed state after the crosslinking process [40,58] and $\bar{v} = 1/\rho_p$ is the hydrogel

specific volume. In this equation the effective number of strands ν_e in the network is expressed as the number concentration of effective strands $\nu_e/V_p = (1 - 2M_c/M)/(\bar{\nu}M_c)$, where V_p is the dry network volume [58]. In Eq. (12) $V_1 \approx 18\ \mathrm{cm}^3/\mathrm{mol}$ is the solvent molar volume. Further, T is the absolute temperature and $Q_e = 1/\nu_2$ is equal to the inverse of the volume fraction of the polymer compound in the swollen network. In Eq. (13), e is the elementary charge, z_i is the charge number of mobile i-ion ($i = 1...N_I$ refer to mobile ions Na^+, H^+, Cl^- and HO^- only), k_B is Boltzmann constant, and C_i^∞ are the molar concentration of mobile ions in the physiological solution far from the hydrogel surface.

It is then clear that in Eq. (10), P_I involves the exchange of solvent and mobile ions between both phases, taking into account that each gelatin chain in the hydrogel has an effective electrical charge Z_p at a given value of pH and I, due to ionizing groups (PVA chains are electrically neutral). P_E and P_S involve the elastic resistance to swelling of the hydrogel network and the mixing process between network and solvent, respectively. It is also clear that as far as the hydrogel surface potential ζ is small, the effective hydrogel charge number Z_p may be obtained from the condition of electroneutrality in both phases far from the interface as follows [4],

$$\sum_{i=1}^{N_I} z_i C_i^\infty \{\exp(-ez_i\zeta/k_BT)\} + Z_pC_p = 0 \tag{14}$$

where $C_p = 1/\bar{\nu}MQ_e$ is the molar concentration of polymer composite in the swollen hydrogel. Further Eqs. (10)–(14) are constrained to satisfy $X_E \approx X - X_C$ as obtained through Eq. (1) or eventually from FTIR (see discussion below). Once experimental values Q_e and M_c at each hydrogel formulation are available, these equations are solved simultaneously to find χ, ζ and $Z_p = Z + X_C$ through an iterative numerical procedure [4].

The knowledge of the hydrogel electrical zeta-potential permits the calculation of the electrical charge density $q = eZ_p/A_oQ_e^{2/3}$ evaluated as follows [4,64],

$$q = 2(2\varepsilon k_BTn^\infty)^{1/2}\sinh\left(\frac{ez_i\zeta}{2k_BT}\right) \tag{15}$$

where n^∞ is the number density of i-free ion and A_o is a characteristic area corrected by the factor $Q_e^{2/3}$ as a consequence of hydrogel swelling. Therefore, $L_1 \approx \sqrt{A_oQ_e^{2/3}M_c/M}$ and $L_2 \approx \sqrt{A_oQ_e^{2/3}}$ are the characteristic electrokinetic lengths associated with the confinements of M_c-chain and M-chains in the hydrogel, respectively [4,65,66].

4. Results and discussion

4.1. Crystal formation in PSG–PVA hydrogels

By following Section 2.6, it was found via FTIR that $f_c^o \approx 61.6\%$ for pure PVA (Fig. 2). This value is consistent with those already reported in the literature. In this regard, one should also observes that PVA hydrogels may be obtained through different procedures [32,67,68], affecting the degree of PVA crystallization. The crystalline PVA mass fraction f_c in samples H-1 to H-11 was calculated via XRD (Section 2.6) as reported in Table 1. These results show that PVA as crosslinker agent of PSG forms crystallites occluded in the hydrogel matrix as a consequence of certain order in the conformation of the monomer pendent –OH groups, thus allowing intra and inter hydrogen bond formations among PVA chains generating crystalline zones [32]. Also f_c increases with higher values of PVA concentrations (higher ratios r) in H-1 to H-11 samples because a higher number of PVA chains are less interfered by PSG chains in the hydrogen bond formations via –OH groups. To better visualize the interplay between chains and crosslinks in the PVA crystallite formation, Figure S1 (b) illustrate, for instance, that the peak in the XRD profile of pure PVA is higher than those of the mixture M-8 and the corresponding hydrogel H-8, indicating that the addition of PSG to PVA inhibit the crystallite formation as a consequence of hindrance effects on hydrogen bonding formations. From this figure, one also concludes through the comparison between M-8 and H-8 peaks of XRD profiles that the amount of discrete crystalline phase in H-8 is lower due to the presence of crosslinks, which are fixing chains and dumping their mobility, to be able to rearrange into crystal domains. For instance, Table S2 shows that $f_c \approx 55.4$ and 49.6% for M-8 and H-8, respectively, which in turns are much lower than $f_c^o \approx 61.6\%$ of the pure PVA. Similar results are obtained for other hydrogels and corresponding mixtures studied here (see also M-1, M-7, H-1 and H-7 in Table S2).

In addition, Figure S1 (b) shows XRD diffractograms in the range $2\theta \approx 7–8^\circ$ corresponding to partial formation of triple-helix tropocollagen conformations of PSG chains, also visualized as crystalline structures [69,70]. In particular the presence of these structures in pure PSG here is a consequence of the rather low drying temperature (see hydrogel preparation in Section 2.4). In this regard, we found experimentally the presence of a diffraction peak at $2\theta \approx 8^\circ$ in the pure PSG (Figure S1 (b)), and also a lower peak in the PSG–PVA hydrogels with $r = 1$ only (samples H-1 and H-2). These results are expected because covalent crosslinks are not present in the pure PSG film and X_C is very low for $r = 1$. On the contrary, in the PSG–PVA mixtures and hydrogels with $r > 1$, both the PVA chain hindrances and esterification reaction (see Table 4) are impeding the tropocollagenic reversion of gelatin chains. It is also clear that molecular structures of gelatin depend on the interactions between water and protein molecules when the water content is above 14% (dry basis). Thus the excess of water molecules reorganizes molecular order by decreasing triple-helix content as reported in Ref. [69]. It should be also observed that samples H-1 to H-11 are in the wet state for the extensional mechanical test (see Section 2.7). Further, these hydrogels are utilized in the wet state as drug and cell carriers, and also for tissue engineering matrices due to their hydrophilic character and capacity to absorb water. Consequently throughout this work it is possible to neglect the small amount of triple-helix structure generated in PSG–PVA hydrogels mainly in samples H-1 and H-2.

Table 3
Hyperelastic parameters G_1, G_2 and G_3 for samples H-1 to H-11, as obtained from the fitting of Eq. (5) to experimental data σ versus λ from simple extensional tests. Also average structural parameters w_c, L_c, N_c and C_n of matrix strands, and average hydrogel mesh size ξ are reported as calculated from the theory described in Section 3.1.

Hydrogel code	G_1 (MPa)	G_2 (MPa)	G_3 (MPa)	w_c (o)	L_c (Å)	N_c	C_n	ξ (Å)
Set I								
H-1	0.018	0.000	0.020	71.1	2.70	351.1	31.38	462.46
H-2	0.000	0.000	0.082	71.1	2.70	267.0	61.87	556.55
H-3	0.112	0.074	0.000[a]	71.1	2.70	190.5	–	–
H-4	0.062	0.094	0.000[a]	71.1	2.70	221.3	–	–
Set II								
H-5	0.040	0.000	0.164	69.3	2.01	203.2	5.23	79.62
H-6	0.070	0.660	0.050	69.3	2.01	86.5	2.99	36.62
H-7	0.120	0.500	0.240	69.3	2.01	85.5	0.52	15.07
Set III								
H-8	0.090	0.900	0.060	70.1	2.32	52.5	2.22	29.94
H-9	0.040	1.360	0.054	69.8	2.21	52.3	0.63	14.44
H-10	0.040	1.360	0.080	69.6	2.13	51.1	0.76	14.72
H-11	0.002	1.800	0.026	69.4	2.07	50.1	0.98	15.95

[a] Experimental data cover the linear and softening responses only. Eq. (5) reduces to the conventional Mooney model with $G_3 = 0$.

The crosschecking of f_c values reported in Table 1 is carried out through DSC tests (Section 2.6). Figure S2 shows DSC profiles of three typical hydrogels (H-1, H-3 and H-4) taking up heat at around 220 °C, which is the PVA melting temperature. Therefore one confirms via DSC that crystalline zones are present in the PSG–PVA hydrogels. Values of f_c thus calculated (see footnote in Table 1) are quite similar to those already found via XRD. Also Figure S3 shows TGA profiles of three typical hydrogels (H-1, H-3 and H-4) where two zones of mass lost are found. One is around 100 °C with a mass dropping of approximately 10%, which may be associated with water evaporation from the hydrogel matrix [33]. The other zone starts at 250 °C with a sharp decrease of sample mass that follows until 320 °C, where the test temperature sweep ends. Thus, it was reported in Refs. [35,71] that around 250 °C, the PVA starts decomposition through different mechanisms and steps. Interesting is the fact that the sample mass is constant around 220 °C in the TGA profile (Figure S3), indicating that at this temperature value there is a melting of PVA crystals without mass lost as indicated in the DSC profile (Figure S2).

4.2. Swelling of PSG–PVA hydrogels

Table 1 also presents experimental values of swelling ratios Q_o, Q_{aw} and Q_e, which are used then in further calculations below. This table shows consistently that hydrogels formulated with a constant PSG concentration (hydrogel Set III) have decreasing swelling ratios with higher PVA concentrations as expected.

This result is a consequence of the formation of hydrogel matrices with a higher crosslink density number, thus limiting the sorption of solvent during the swelling process. The same hydrogel responses are found for the ratios $r = 1$ and 4 corresponding to hydrogel Sets I and II, respectively. Further when r is kept constant by increasing both PSG and PVA amounts, a higher crosslink density number is obtained once more, although this evolution becomes saturated at high concentrations due to chain hindrance effects on the remaining sites $(X - X_C)$ available for further crosslinks. The onset of these effects also occurs when X_C becomes approximately constant as discussed below (see Section 4.4 and Table 4). The description of Table 1 provides the maximum standard deviations (±SD) typically found in the experimental procedure. The higher standard deviations are obtained for H-1 to H-4 with $r = 1$ (hydrogel Set I), having low number of crosslinks, and hence high swelling ratio values, which generate major difficulties in the conditioning of hydrogel surface before weighing to get W_w values [4].

Table 4
Stoichiometric fractions X_C and X_E obtained from mechanical characterization (minimum number of covalent crosslinks and maximum number of remaining carboxylic groups, respectively), electrokinetic parameters χ, ζ and Z_p obtained from swelling parameters and average molecular mass of network strands, and characteristic scales L_1 and L_2 calculated for samples H-1 to H-11.

Hydrogel code	X_C	X_E	χ	ζ (mV)	Z_p	L_1(Å)	L_2 (Å)
Set I							
H-1	2.4	69.3	0.528	0.34	3.10	217	403
H-2	3.5	68.2	0.525	0.49	4.18	184	392
H-3	5.3	66.4	0.543	1.14	6.00	122	308
H-4	4.5	67.2	0.557	1.15	5.12	121	282
Set II							
H-5	6.7	65.0	0.577	1.91	7.33	95	262
H-6	17.0	54.7	0.598	5.65	17.66	56	237
H-7	17.2	54.5	0.600	5.88	17.88	55	233
Set III							
H-8	25.3	46.4	0.576	7.11	25.96	50	255
H-9	26.5	45.2	0.594	8.63	27.19	45	237
H-10	28.1	43.6	0.603	9.66	28.75	43	230
H-11	29.5	42.2	0.606	10.31	30.11	41	228

It is relevant to visualize that the reference state of deformation of hydrogels is associated with the swelling ratio Q_o in Eqs. (8) and (11). Thus hydrogel isotropic deformations at equilibrium after the swelling process are expressed either through Q_{aw}/Q_o and Q_o/Q_e when the water–ethanol and physiological solutions are used, respectively. Although the equilibrium swelling states Q_{aw} and Q_e are independent from the swelling paths considered to reach them, we have observed that dry hydrogels are anisotropic as it was found via dimension measurements before and after the swelling process. This phenomenon does not require consideration here because the reference state is taken at the swelling ratio Q_o [40].

For practical reasons and to avoid scattering error amplifications, experimental values Q_o, Q_{aw} and Q_e as a function of m_{PVA} are fitted through simple equations (correlation coefficients higher than 0.98 are obtained) to evaluate the Q_{aw}/Q_o and Q_o/Q_e ratios used then in Eqs. (8) and (11).

4.3. Simple extension of PSG–PVA hydrogels

The stress response of PSG–PVA hydrogels in simple extension permits the evaluation of shear modulus G through Eq. (8), apart from other mechanical properties analyzed below. Therefore this equation requires the estimation of $\phi = \phi^c_{PVA}/Q_{aw}$ in the hydrogel matrix plasticized with water–ethanol solution before the extension test (see Sections 2.5 and 2.7). In Table 2 one observes that ϕ mainly increases with lower values of Q_{aw}, and higher values of m_{PVA}, or equivalently for higher ratio r, as expected. Also this table shows that in general the shear modulus for samples H-1 to H-11 increases consistently with higher concentration of PVA, except for the samples (H-3, H-4) of Set I. Here it is clear that H-4 has the higher PSG concentration and hence this sample is not able to crosslink effectively for the same PVA concentration as that of PSG due to the overcrowding of chains at these high concentrations (see also Section 4.4).

Figure S4 depicts the fittings of experimental data through Eqs. (5) and (7) for hydrogel Set I (H-1 to H-4). The maximum average error is less than 6.9% indicating rather good model performances. This error is calculated through $\sum_{i=1}^{i=J}|(\sigma_i^{exp} - \sigma_i^m)/((J\sigma_i^{exp})|$, where J is the number of experimental points and σ_i^{exp} and σ_i^m are the experimental and fitted stresses, respectively, both at a given experimental stretch ratio. In this Set I the mass ratio is kept constant at $r = 1$, and Figure S4 shows that as the concentrations of both PVA and PSG increases, the stress response of these samples may switch from linear-hardening response (BST model applies to H-1 with $m_{PSG} = 2.5$ g and H-2 with $m_{PSG} = 5$ g) to lineal-softening response only (worm-like model applies satisfying asymptotically the conventional Mooney model, at H-3 with $m_{PSG} = 10$ g and H-4 with $m_{PSG} = 12.5$ g) as a consequence that these samples are rather fragile (low deformation onset at fracture). Here the Mooney model is obtained with the worm-like hyperelastic model when $G_3 = 0$ (see Eq. (5) and Tables 2 and 3).

Fig. 4 depicts the fitting of Eq. (5) to experimental data obtained through the simple extensional test for hydrogel Set II (H-5 to H-7). The average error is less than 6.7% indicating a good model performance again. For this case the mass ratio is kept constant at $r = 4$, and this figure shows that as the concentrations of both PVA and PSG increase, the stress response of these samples switches from linear-hardening response (here worm-like hyperelastic model applies to H-5 with $m_{PSG} = 1.25$ g and $G_2 = 0$) to lineal-softening-hardening response (here worm-like hyperelastic model applies to H-6 with $m_{PSG} = 2.5$ g and H-7 with $m_{PSG} = 3$ g and $G_2 \neq 0$). Therefore, when r is relatively high, the onset of chain reptation appears [54] (onset of softening response). This specific phenomenon is a consequence of the matrix topological constraints

imposed to strand deformations causing a shift of the hydrogel hardening response toward higher stretch ratios.

Figure S5 depicts the fitting of Eq. (5) to experimental data obtained through the simple extensional test for hydrogel Set III (H-8 to H-11). The average error is less than 6.4% indicating once more a good model performance. Thus, for $r = 2$, 2.5, 3 and 3.5 the worm-like hyperelastic model applies for these samples with $m_{PVA} = 10$, 12.5, 15 and 17.5 g, respectively. The ratio $r = 3$ for H-10 is not shown in this figure to improve curves visualizations only. In Figure S5, the response of H-2 is also added (it should be observed that this sample may be classified in both Sets I and III) which has $m_{PSG} = 5$ g with mass ratio $r = 1$ and is fitted better by the BST hyperelastic model as indicated in Table 2.

In particular the linear-hardening responses of H-1 and H-2 presented through Figures S4 and S5 are fitted better with the BST model (Eq. (7)) than with the worm-like hyperelastic model (Eq. (5)). For instance, for H-2 the average errors are 2.5 for the former and 4.2% for the later. Nevertheless, the BST model does not provide information on topological parameters of the crosslinked matrix as in the case that the worm-like hyperelastic model is used. Since these topological parameters are useful for calculations in Section 3.1, mainly in the estimation of the average C_n values of chains in the matrix, we decided to fit all the experimental data σ versus λ of hydrogel sets with Eq. (5) as indicated in Tables 2 and 3. These tables show the relevance of characterizing mechanically the PSG-PVA hydrogels, from which the values of the following parameters G, M_c, β, n, T_H, G_1, G_2 and G_3 are obtained by using the theory described in Section 3.1.

Table 2 also shows values of Hencky toughness for the three hydrogel sets. Thus PSG–PVA hydrogels with the lower mass ratios (Set I with $r = 1$) have quite low T_H because the relative PVA mass is not enough to crosslink appropriately the PSG chains. This table also shows consistently that Set I has the higher values of molecular mass between two consecutive crosslinks M_c indicating lower crosslink density number. These undesired properties were enhanced for $r < 1$; for instance, hydrogel samples formulated with $r = 0.06$ and 0.2 yielded shear modulus values 0.007 and 0.017 MPa and toughness values 0.004 and 0.011 MPa, respectively. The hydrogel toughness is improved when $r > 1$ as depicted in Table 2. In this regard, we found that the higher value of T_H is around 8 MPa for H-7 with $m_{PSG} = 3$ g and $m_{PVA} = 12$ g, indicating that in order to get high toughness the mass of the desired polyampholytic component must be lower than the PVA mass used as crosslinker. On the other hand, to promote drug-hydrogel ion complexations as discussed in Section 1, an appreciable amount of PSG is required. In this case hydrogel Set III (H-8 to H-11), with $2 < r < 3.5$, provides T_H in the range of high values (from around 2–7.8 MPa) with a matrix electrical state still favorable for the design of hydrogel purposes (see Section 4.4 and H-8 to H-11 in Table 4). In addition concerning the final mechanical responses of PSG–PVA hydrogels, it should be observed that apart from its preferred high toughness (high energy storage under deformation) the condition of appropriate deformability is also a target. For this purpose the experimental stretch ratio at fracture is reported in Table 2 indicating that once more the best hydrogel deformability is achieved with Sets II and III. Further from this point of view probably one would prefer, for instance, hydrogel H-11 with $r = 3.5$ and $m_{PSG} = 5$ g having $T_H \approx 6.68$ MPa, $\lambda_F \approx 4.81$ and relatively high PSG chain cationization (see also below concerning the hydrogel electrical state).

From the fitting of experimental σ versus λ with Eq. (5), dimensionless β values are obtained. Table 2 shows that for the full set of samples studied here, this parameter varies from very low values of order 10^{-2} for H-7 (high PVA concentrations with $r = 4$) to high values around 0.35 for H-2 (low PVA concentrations with $r = 1$). By taking into account that hydrogels were formulated with two different types of chains, these results were consistent with those found in Ref. [37] studying different networks, where lower β values were found for matrices of natural rubber or synthetic networks while higher β values belonged to biological networks with rather more extended strands ($\beta \to 1$). In addition, here hydrogel shear moduli followed a trend inverse to that of β parameter as already found in Ref. [37]. In fact, since our hydrogels include biopolymer PSG chains, the responses for G and β described above as a function of ratio r are expected (see Tables 1 and 2). Thus, sample H-11 with $m_{PVA} = 17.5$ g and $m_{PSG} = 5$ g yields $G = 1.828$ MPa and $\beta = 0.029$, while sample H-2 with $m_{PVA} = 5$ g and $m_{PSG} = 5$ g has $G = 0.082$ MPa and $\beta = 0.350$, validating the above analysis. In the last sample it is evident that less covalent crosslinks are found resulting in a lower shear modulus and stiffer strands (high persistence length [37,54]). By following these relevant physical aspects, for the case the samples have the same amounts of PVA and different amounts of PSG, like H-6 and H-8 with $m_{PSG} = 2.5$ g and $m_{PSG} = 5$ g, respectively (Table 2), one finds that β is higher for H-8 as expected, because it contains the higher biopolymer concentration.

Consistently with the above results C_n values are calculated from β as reported in Table 3. We found that samples H-1 and H-2 of Set I with $r = 1$ do not show a significant softening response in simple extension (Figure S4). Also their σ versus λ relationship can be fitted by the BST model even with a good correlation coefficient. The physical consequence is that these samples present the higher C_n when Eq. (5) is used. In fact, when the concentrations of PSG and PVA are substantially increased (see H-3 and H-4 in Figure S4) still by keeping $r = 1$, the softening zone appears but the samples break before reaching the hardening zone. This last response impede the evaluation of C_n because the worm-like hyperelastic model Eq. (5) reduces to Mooney model with $G_3 = 0$ in order to be able to fit experimental data σ versus λ. Also the BST is not applicable anymore here. It is then clear that Set I is in general too low in shear modulus, fracture stretch ratio, toughness (see Table 2 and discussion above), crosslinking density and PSG chain cationization (see Table 4, and description below). These results clearly indicate that r must be increased to improve the mechanical and electrokinetic performance of H-1 to H-4 hydrogels. On the other hand Sets II and III present lower C_n as a consequence of increasing r and hence PVA concentrations. Nevertheless, one should observe here that C_n values are approximations allowing a qualitative analysis of a rather complex crosslinked heterochain network. It is also clear that the statistical definition of C_n is rather biased by the presence of crosslinks that are shortening network strands.

The next step in the PSG–PVA hydrogel characterization is concerned with the estimation of the average matrix mesh size. In fact, relative values ξ for different hydrogel formulations are needed, even in the case these values are estimations through scaling theories (Section 3.1). Table 3 reports ξ values for hydrogel formulations except for H-3 and H-4 with $m_{PSG} = 10$ and 12.5 g, respectively, which have $G_3 = 0$. This means very high ξ values giving a mesh size of the order of the primitive chain. To visualize the calculations carried out here, this table also provides the evaluation of average structural parameters of matrix strands, w_c, L_c, N_c and C_n, obtained through expressions provided in Section 3.1. The lower ξ values belong to hydrogel Set III, where $m_{PSG} = 5$ g with $r = 2$ to 3.5, indicating that within this set one may find good mechanical properties as shown above and also relatively small interstices in the matrix to impede a rapid drug release through pure diffusion. On the contrary, it may be inferred that hydrogel Set I is prone to produce a sudden and high drug diffusion flux at short release times (initial burst effect [7]), which lower the efficacy of the drug therapy, mainly when the biodegradation shall be the main mechanism for release.

4.4. Electrokinetic properties of PSG–PVA hydrogels

Within the basic characterization process of PSG–PVA hydrogels, some relevant electrokinetic parameters and stoichiometric fractions already discussed in Sections 2.3 and 3.2 must be provided. Thus Table 4 illustrates that X_C for a fixed r increases with the amount of PVA (hydrogel Sets I and II) as one expects (concerning H-3 and H-4 see also discussion in Section 4.3). For hydrogel Set III this table shows that at a fixed PSG mass of 5 g, the increase of PVA produces a raise in the crosslink number X_C. The numerical procedure indicated in Section 3.2 through Eqs. (10)–(14) also provides the effective electrical charge number Z_p of PSG chains in the hydrogel as one of the relevant electrokinetic parameters. It is thus found that the hydrogel Set III provides the higher values of Z_p indicating that crosslinker PVA yields a high cationization of basic PSG chains. This effect is relevant to achieve ion complexation between negative drug molecules and hydrogel matrix when the released is planned via matrix biodegradation, as for instance occurs with the controlled release of heparin Ref. [12]. Values of the electrokinetic parameters χ and X_E are also reported in Table 4 to better visualize the consistency of calculations, taking into account that they are a direct result from the expressions reported in Section 3.2. Interesting is the fact that hydrogel formulations studied here have small zeta potentials ζ not exceeding 11 mV. This result is a favorable electrostatic aspect of these hydrogels because one should not expect complex polarization phenomena of the charged drug diffusing into the matrix during the loading process. Furthermore when samples H-1 to H-11 are equilibrated in 3.5 ml of physiological solution (Tables 1 and 4) the pH in these hydrogels (designated pH^*) is in the range 7–7.2 corresponding to zeta potential values between 0.34 and 10.31 mV (Table 4). In fact, hydrogen ion equilibration implies $pH^* \approx pH + e\zeta/(\ln(10)k_BT)$ (see details in Refs. [4] and [72,73]). Table 4 indicates that the smaller scales of confinements L_1 and L_2 of the electrically charged PSG chains in the swollen hydrogel matrix belongs to Set III consistently with the parameter values reported above. They are useful to estimate the size of basic electrostatic patches where ion complexation between PSG and charged drug may occur (see also Ref. [4] concerning gelatin-GTA hydrogels).

4.5. Validation of covalent –COOC– sites formed in PSG–PVA hydrogels

In relation to –COOC– sites formed in the crosslinking process, it is clear that the theoretical framework for the characterization of PSG–PVA hydrogels depends on the average number of –COOH groups per PSG chain. Therefore, it is relevant to validate via FTIR the X value estimated from the AAS (Table S1). In this regard, it was found that $X \approx 72.5$ as obtained from the digitalization of curve b in Fig. 2 and also the use of $A(\nu) = A(1718)$ in the method described in Section 2.6, which is close to value $X \approx 71.7$ already found from calculations reported in Table S1. Also it is important to validate the estimation of X_C obtained through Eq. (1) by taking into account that the matrix may have defects yielding elastically non-effective crosslinks, which cannot support elastic stress. Therefore, for this purpose three different hydrogels and corresponding mixtures were chosen to be tested via FTIR (H-1, H-7 and H-8 and M-1, M-7 and M-8, respectively). The spectra are already shown in Fig. 3 and the X_C obtained are reported in Table 5 (see also procedure in Section 2.6). It is clear that X_C obtained via FTIR are slightly higher than those found through Eq. (1). These results however have a simple explanation. In fact, hydrogel stress responses to extension tests are sensitive to elastically effective network crosslinks only. Although Eq. (1) is already corrected by terminal chain ends on the average, the network may still presents other imperfections like dangling chain crosslinks, justifying the rather small differences pointed out above. Nevertheless, as far as the ratio $r > 1$ yielding a satisfactory amount of crosslinks one may conclude that Eq. (1) is a good and practical estimation of X_C. In this regard, Table 5 also presents values of Z_p and ζ calculated from X_C as obtained via FTIR. These values are quite conservative to validate results in Table 4.

Table 5
Stoichiometric fractions X_C and X_E obtained from FTIR spectra (approximate actual number of covalent crosslinks and number of remaining carboxylic groups, respectively), actual electrokinetic parameters ζ and Z_p obtained from swelling parameters, average molecular mass of network strands and actual X_C, for samples H-1, H-7 and H-8.

Hydrogel code	X_C	X_E	ζ (mV)	Z_p
H-1	6.4	66.1	0.78	7.07
H-7	18.0	54.5	6.12	18.65
H-8	27.4	45.1	7.66	28.01

5. Conclusions

From these analyses and calculations it is shown that polyampholyte PSG–PVA hydrogels may be well designed for the controlled release of charged drug molecules via biodegradation of the heterochain network matrix, during a biocompatible and no citotoxic process. More specifically the estimation of physicochemical (Q_e and Q_{aw}), mechanical (G, T_H and λ_F), morphological (M_C and ξ), and electrokinetic (Z_p, ζ, L_1 and L_2) hydrogel properties and scales provide a valuable information mainly for hydrogel manipulation, drug-matrix polyion complexation, drug loading and release of therapeutic charged molecules via hydrogel biodegradation. In these regards, samples H-7 to H-11 seem to be the more appropriate ones having high modulus, toughness and PSG chain cationization. Within this framework, future researches may use these characterization results to study the loading and release mechanisms of effectively negative charged drugs in PSG–PVA hydrogels involving specific applications already proposed in modern literature.

Acknowledgments

Authors wish to thank the financial aid received from Universidad Nacional del Litoral, Santa Fe, Argentina (CAI+D 2009) and CONICET (PIP 112-200801-01106).

Appendix A. Supplementary data

Supplementary data related to this article can be found at http://dx.doi.org/10.1016/j.polymer.2013.03.045.

References

[1] Veis A. The macromolecular chemistry of gelatin. 1st ed. New York: Academic Press, Inc.; 1964 [chapter III].
[2] Ward AG, Courts A. The science and technology of gelatin. 1st ed. London: Academic Press, Inc.; 1977.
[3] Ledward DA. Gelatin of gelatins. In: Mitchell JR, Ledward DA, editors. Functional properties of food macromolecules. New York: Elsevier Applied Science Publishers; 1986. p. 171–201.
[4] Deiber JA, Ottone ML, Piaggio MV, Peirotti MB. Polymer 2009;50(25):6065–75.
[5] Tabata Y, Hijikata S, Ikada Y. J Control Release 1994;31(2):189–99.
[6] Yamada K, Tabata Y, Yamamoto K, Miyamoto S, Nagata I, Kikuchi H, et al. Neurosurgery 1997;86(5):871–5.
[7] Tabata Y, Ikada Y. Adv Drug Deliv Rev 1998;31(3):287–301.
[8] Young S, Wong M, Tabata Y, Mikos AG. J Control Release 2005;109(1–3):256–74.
[9] Malafaya PB, Silva GA, Reis RL. Adv Drug Deliv Rev 2007;59(4–5):207–33.
[10] Huang S, Fu X. J Control Release 2010;142(2):149–59.
[11] Hwang J, Kim I, Lee JY, Piao S, Lee DS, Lee TS, et al. Biomaterials 2011;32(19):4415–23.
[12] Saito T, Tabata Y. Acta Biomater 2012;8(2):646–52.
[13] Ozekp M, Ishii T, Hirano Y, Tabata Y. J Drug Target 2001;9(6):461–71.

[14] Oe S, Fukunaka Y, Hirose T, Yamaoka Y, Tabata Y. J Control Release 2003;88(2):193–200.
[15] Tabata Y, Yamamoto M, Ikada Y. Pure Appl Chem 1998;70(6):1277–82.
[16] Tabata Y, Ikada Y. Biomaterials 1999;20(22):2169–75.
[17] Hori K, Sotozono C, Hamuro J, Yamasaki K, Kimura Y, Ozeki M, et al. J Control Release 2007;118(2):169–76.
[18] Kodama N, Nagata M, Tabata Y, Ozeki M, Ninomiya T, Takagi R. Bone 2009;44(4):699–707.
[19] Narita A, Takahara M, Ogino T, Fukushima S, Kimura Y, Tabata Y. The Knee 2009;16(4):285–9.
[20] Ratanavaraporn J, Furuya H, Kohara H, Tabata Y. Biomaterials 2011;32(11): 2797–811.
[21] Fukunaka Y, Iwanaga K, Morimoto K, Kakemi M, Tabata Y. J Control Release 2002;80(1–3):333–43.
[22] Kushibiki T, Tomoshige R, Fukunaka Y, Kakemi M, Tabata Y. J Control Release 2003;90(2):207–16.
[23] Ofner III CM, Bubnis WA. Pharm Res 1996;13(12):1821–7.
[24] Strauss G, Gibson SM. Food Hydrocolloids 2004;18(1):81–9.
[25] Chen Y, Chang J, Cheng C, Tsai F, Yao C, Liu B. Biomaterials 2005;26(18):3911–8.
[26] Cao N, Fu Y, He J. Food Hydrocolloids 2007;21(4):575–84.
[27] Pal K, Banthia AK, Majumdar DK. AAPS Pharm Sci Tech 2007;8(1):E1–5.
[28] Hoare TR, Kohane DS. Polymer 2008;49(8):1993–2007.
[29] Lien S, Li W, Huang T. Mater Sci Eng C Mater Biol Appl 2008;28(1):36–43.
[30] Gander B, Gurny R, Doelker E, Peppas NA. Pharm Res 1989;6(7):578–84.
[31] Peppas NA, Mongia NK. Eur J Pharm Biopharm 1997;43(1):51–8.
[32] Hassan CM, Peppas NA. Adv Polym Sci 2000;153(1):37–65.
[33] Hassan CM, Peppas NA. Macromolecules 2000;33(7):2472–9.
[34] Hassan CM, Stewart JE, Peppas NA. Eur J Pharm Biopharm 2000;49(2):161–5.
[35] Juntanon K, Niamlang S, Rujiravanit R, Sirivat A. Int J Pharm 2008;356(1–2):1–11.
[36] Blatz PJ, Sharda SC, Tschoegl NW. Trans Soc Rheol 1974;18(1):145–61.
[37] Dobrynin AV, Carrillo J- MY. Macromolecules 2011;44(1):140–6.
[38] Gupta S, Pramanik AK, Kailath A, Mishra T, Guha A, Nayar S, et al. Colloids Surf B Biointerfaces 2009;74(1):186–90.
[39] Bigi A, Cojazzi G, Panzavolta S, Rubini K, Roveri N. Biomaterials 2001;22(8): 763–8.
[40] Peppas NA, Merril EW. J Polym Sci Part A Polym Chem 1976;14(2):441–57.
[41] Peppas NA. Die Makromol Chem 1977;178(2):595–601.
[42] Mansur HS, Sadahira CM, Souza AN, Mansur AAP. Mater Sci Eng C Mater Biol Appl 2008;28(4):539–48.
[43] Assender HE, Windle AH. Polymer 1998;39(18):4295–302.
[44] Assender HE, Windle AH. Polymer 1998;39(18):4303–12.
[45] Kaczmarek H, Podgórski A. J Photochem Photobiol A Chem 2007;191(2–3): 209–15.
[46] Costa-Júnior ES, Barbosa-Stancioli EF, Mansur AAP, Vasconcelos WL, Mansur HS. Carbohydr Polym 2009;76(3):472–81.
[47] Focher B, Beltrame PL, Naggi A, Torri G. Carbohydr Polym 1990;12(4):405–18.
[48] Minus ML, Chae HG, Kumar S. Polymer 2006;47(11):3705–10.
[49] Lai G, Du Z, Li G. Korea–Australia Rheol J 2007;19(2):81–8.
[50] Hoque MS, Benjakul S, Prodpran T. Food Hydrocolloids 2011;25(1):82–90.
[51] Flory PJ. Principles of polymer chemistry. 9th ed. London: Cornell University Press; 1975 [chapter XI].
[52] Mark JE, Erman B. Molecular aspects of rubber elasticity. In: Stepto RFT, editor. Polymer networks. NewYork: Blackie Academic&Professional; 1998. p. 215–42.
[53] Shibayama M, Tanaka T. Adv Polym Sci 1993;109(1):1–62.
[54] Rubinstein M, Colby RH. Polymer physics. 1st ed. Oxford: Oxford University Press; 2004 [chapter VII].
[55] Flory PJ. Statistical mechanics of chain molecules. 1st ed. New York: Interscience Publishers; 1969.
[56] Mwangi JW, Ofner III CM. Int J Pharm 2004;278(2):319–27.
[57] Lin C-C, Metters AT. Adv Drug Deliv Rev 2006;58(12–13):1379–408.
[58] Brannon-Peppas L, Peppas NA. Chem Eng Sci 1991;46(3):715–22.
[59] Mafé S, Manzanares JA, English AE, Tanaka T. Phys Rev Lett 1997;79(16): 3086–9.
[60] English AE, Tanaka T, Edelman ER. Macromolecules 1998;31(6):1989–95.
[61] English AE, Tanaka T, Edelman ER. Polymer 1998;39(24):5893–7.
[62] Eichenbaum GM, Kiser PF, Dobrynin AV, Simon SA, Needham D. Macromolecules 1999;32(15):4867–78.
[63] Huang Y, Szleifer I, Peppas NA. Macromolecules 2002;35(4):1373–80.
[64] Russell WB, Saville DA, Schowalter WR. Colloidal dispersions. 1st ed. Cambridge: Cambridge University Press; 1989 [chapter IV].
[65] Dobrynin AV, Zhulina EB, Rubinstein M. Macromolecules 2001;34(3):627–39.
[66] Dobrynin AV, Colby RH, Rubinstein M. J Polym Sci Part B Polym Phys 2004;42(19):3513–38.
[67] Hickey AS, Peppas NA. J Membr Sci 1995;107(3):229–37.
[68] Mallapragada SK, Peppas NA. J Polym Sci Part B Polym Phys 1996;34(7):1339–46.
[69] Yakimets I, Wellner N, Smith AC, Wilson RH, Farhat I, Mitchell JR. Polymer 2005;46(26):12577–85.
[70] Yakimets I, Paes SS, Wellner N, Smith AC, Wilson RH, Mitchell JR. Biomacromolecules 2007;8(5):1710–22.
[71] Holland BJ, Hay JN. Polymer 2001;42(16):6775–83.
[72] Piaggio MV, Peirotti MB, Deiber JA. Electrophoresis 2005;26(17):3232–46.
[73] Piaggio MV, Peirotti MB, Deiber JA. Electrophoresis 2009;30(13):2328–36.